A re-assessment of the nitrogen geochemical behavior in upper oceanic crust from Hole 504B: Implications for subduction budget in Central America

Vincent Busigny[1,2], Pierre Cartigny[1], Christine Laverne[3], Damon Teagle[4], Magali Bonifacie[1], Pierre Agrinier[1]

[1] *Institut de Physique du Globe de Paris, Sorbonne Paris Cité, Univ. Paris Diderot, UMR 7154 CNRS, 1 rue Jussieu, 75238 Paris, France*

[2] *Institut Universitaire de France, Paris, France*

[3] *Laboratoire de Pétrologie Magmatique, Case 441, Université Paul Cézanne Aix-Marseille III, Faculté des Sciences et Techniques, Avenue Escadrille Normandie Niemen, 13397 Marseille Cedex 20, France*

[4] *School of Ocean and Earth Science, National Oceanography Centre Southampton, University of Southampton, Southampton, SO14 3ZH, UK*

Corresponding author: busigny@ipgp.fr

Keywords: nitrogen, isotopes, oceanic crust, subduction, hydrothermal

Abstract

The geochemical behavior of N during seawater-oceanic crust alteration remains poorly constrained. Yet, it is a central parameter to assess the flux of N to subduction zones. Most studies proposed that hydrothermally altered basaltic rocks are enriched in N relative to fresh basalts. However, published data from DSDP/ODP Hole 504B, a reference site for the composition of the oceanic crust, suggest that seawater alteration leads to the N depletion of the upper ocean crust. To better address this issue, we analyzed N concentration and isotope composition of 21 altered basalts from the lavas and sheeted dikes sampled by Hole 504B. These new analyses show significant N enrichment (up to 14.1 ppm) relative to fresh degassed MORB (~1 ppm). The differences observed between earlier and modern data are interpreted as resulting from analytical artifact due to the earlier use of a molybdenum crucible for N extraction. Furthermore, our new data show a progressive decrease of N concentration with depth, from 14.1 to 1.4 ppm. Nitrogen isotope compositions display a large range, with $\delta^{15}N$ values from -0.9 to +7.3‰, and most likely reflect multiple stages of alteration with fluids of various compositions. In contrast to N concentration, $\delta^{15}N$ values do not show a global depth trend but oscillate around a mean value of 3.0 ± 2.2 ‰ (1SD). The N concentration shows a positive correlation with bulk rock $\delta^{18}O$ values, suggesting that N behavior during alteration process is mainly controlled by temperature. We propose that N speciation in the hydrothermal fluid is dominated by NH_3/NH_4 at low temperature (<200°C) but is transformed to N_2, associated with H_2, at higher temperature (>200°C). These new data are used to re-evaluate the global flux of N input into Central American subduction zone, showing that the upper basaltic crust represent about 20% of the total N buried in subduction zone. A comparison with previous results obtained on N degassed in volcanic arc illustrates that, in "warm" subduction zone like Central America, up to 50% of the subducted N may be transferred to the deep mantle. This contrasts with "cold" subduction environments, where >80% of the N inputs escape sub-arc slab devolatilization and supports that the geothermal gradient plays a major role in determining the N fate in subduction zones.

61

62 **1. Introduction**

63

64 Hydrothermal circulation systems associated with mid-ocean ridges profoundly influence the
65 chemistry of the oceanic crust (*e.g.* Alt, 1995; Alt and Teagle, 2000). Understanding these
66 systems is crucial to unravel the chemical evolution of the ocean, the oceanic crust and
67 ultimately the mantle, which is affected by inputs from subducting-slabs. It is well accepted
68 that the upper oceanic crust acts as a significant sink for elements such as K, Mg, Rb, Cs, B,
69 Li, U, CO_2 and H_2O, while it is a source for Ca and Si (*e.g.* Alt, 1995; Alt et al., 1996a, 1996b;
70 Laverne et al., 2001; Staudigel, 2003; Bach et al., 2003). Some elements like N, for which
71 analysis is technically challenging, still have uncertain geochemical behavior.
72 Only few studies have focused on the N exchanges during fluid-induced alteration of basalts
73 (Hall, 1989; Erzinger and Bach, 1996; Busigny et al., 2005a; Li et al., 2007; Bebout et al.,
74 2018). In an early contribution, Hall (1989) estimated the N content of spilitized basalts from
75 the Cornubian massif (Southwest England) and suggested that N was enriched in rocks during
76 alteration processes. However, whether spilitic alteration of Cornubian basalts could be
77 considered as representative of oceanic crust processes in general remains uncertain. Nitrogen
78 content determination in subsequent studies of oceanic basalts from several DSDP/ODP Sites
79 (Busigny et al., 2005a; Li et al., 2007) and from Mesozoic ophiolites (Bebout et al., 2018)
80 supported the interpretation of N enrichment but showed smaller magnitude than basalts from
81 Cornubian massif. The analysis of altered basalts from DSDP/ODP Hole 504B contrasted
82 with these results, and pointed to a loss of N from rock to fluid (Erzinger and Bach, 1996).
83 The different results obtained on samples from DSDP/ODP sites were suggested to originate
84 either from different types of alteration processes or analytical discrepancies between the
85 various studies (Busigny et al., 2005a). In their study of Hole 504B basalts, Erzinger and Bach
86 (1996) extracted N using a pyrolysis technique, heating the samples in a molybdenum
87 crucible. However, later experiments demonstrated that N is strongly adsorbed by
88 molybdenum even at high temperature (Yokochi et al., 2006). The low N concentration

measured in Hole 504B altered basalts may thus result from incomplete recovery of N rather than a specific type of alteration.

In the present contribution, we conducted new analyses of altered basalts and dolerites from Hole 504B to evaluate the behavior of N during hydrothermal alteration and evaluate potential analytical artifacts in previously published results. Nitrogen contents and isotopic compositions were measured for 21 samples recovered at various depths, from 317.2 to 1830.4 meters below seafloor (mbsf) of the upper oceanic crust. These new results confirm the general N enrichment during oceanic crust alteration. Additionally, the combination of these new N data with major and trace element concentrations and bulk O isotope compositions is used to better constrain N geochemical behavior during alteration of the upper crust. A global mass balance approach is presented to evaluate the contribution of upper oceanic crust to the subducted N in Central America.

2. Geological background and sample description

Hole 504B has been extensively studied within the last 40 years and is generally considered as a reference site for the structure, petrology and composition of upper oceanic crust. It is located in the eastern equatorial Pacific in the Panama basin, 200 km south of the intermediate spreading rate Costa Rica Rift (Fig. 1). It lies on ~ 6 Ma oceanic lithosphere under 3474 m of water. The drilled section is the deepest within oceanic crust and reaches 2111 meters below seafloor (mbsf). The lithostratigraphy of Hole 504B (Fig. 2) is characterized by (i) 274.5 m of sediments (siliceous oozes, chert, limestone and chalk), (ii) a 571.5 m-thick volcanic section including pillow lavas, massive flows, and breccias with local dikes in the lower half of the section, (iii) a 209 m-thick transition zone of lavas and dikes, underlain by (iv) 1056 m of sheeted dike complex (Alt et al., 1986a, 1986b, 1996a). The section collected at Hole 504B has been further divided into five hydrothermal alteration zones based on secondary mineral assemblages and bulk-rock chemical compositions (see review in Alt et al, 1996a). These five zones, from top to bottom, are:

(1) The Upper Pillow Alteration Zone (UPAZ), from 274 to 594 mbsf, exhibits three types of alteration (Honnorez et a., 1983; Alt et al., 1996b). The first type corresponds to the slightly altered background dark grey rocks that occur throughout the volcanic section with smectite (Mg-saponite) as the dominant secondary mineral. These rocks are interpreted to result from low temperature seawater/basalt exchanges at low water/rock ratio. The other two styles of alteration occur as halos adjacent to veins and include (i) "black halos", characterized by the presence of celadonite, a K-bearing mica, and (ii) "brown oxidized halos" which can exhibit various shades of brown, red and orange, due to the presence of iron-oxyhydroxides reflecting the effect of a low temperature (<110°C) oxidative alteration process (Alt et al., 1996a).

(2) The Lower Pillow Alteration Zone (LPAZ) extends from 594 to 846 mbsf. In this zone, basalts contain no alteration halos adjacent to veins. They display a uniform dark grey color, with smectite and pyrite representing the dominant secondary minerals. The alteration conditions are interpreted as non-oxidative with more restricted fluid circulation and temperatures up to 150°C.

(3) The Mineralized Zone (MZ), from 846 to 1055 mbsf, contains highly fractured, brecciated pillows and dikes. This zone records the transition from low-temperature alteration (<150°C) and higher temperature hydrothermal alteration (> 250°C) with the appearance and then increasing abundance with depth of greenschist facies minerals. Four successive stages of alteration have been deduced from secondary minerals relationships in veins and crosscutting veins (following Alt et al., 1986b): (1) chlorite, actinolite, albite-oligoclase and titanite formed at 200°C to >300°C from reaction with seawater-derived hydrothermal fluids; (2) quartz, epidote and sulfides at 250°C-380°C from highly reacted, evolved hydrothermal fluids; (3) anhydrite, resulting from the recharge of hydrothermal system by seawater; and (4) zeolites, prehnite and calcite, formed at temperature <250°C by evolved hydrothermal fluids. A Cu-rich mineralized stockwork zone occurs at 910-918 mbsf (Honnorez et al., 1985).

(4) The Upper Dikes (UD) extend from 1055 to 1500 mbsf, and are characterized by secondary minerals and alteration sequence similar to those of the Mineralized Zone (MZ). The intensities of hydrothermal alteration and recrystallization of the UD are highly variable and depend on the fracturing and permeability of the rocks.

146 (5) The Lower Dikes (LD) range from 1500 to 2111 mbsf. They generally show the same
147 alteration stages than the Mineralized Zone (MZ) and Upper Dikes (UD), except an early
148 high-temperature alteration stage (>400°C) that preceded the stages described in the UD. This
149 stage is characterized the presence of secondary calcic plagioclase and Mg-hornblende
150 (Vanko and Laverne, 1998). It is interpreted as resulting from calcium-enriched hydrothermal
151 fluids present in the reaction zone, between the hydrothermal system and the magmatic
152 chamber at the bottom of the dike section.
153 Overall, the various rocks from Hole 504B thus record a complex multi-stage alteration
154 history (*e.g.* Alt et al., 1996a). They are characterized by increasing alteration temperatures
155 and decreasing water/rock ratios with depth (Friedrichsen et al., 1985; Alt et al., 1986a;
156 Kawahata et al., 1987; Kusakabe et al., 1989; Agrinier et al., 1995; Teagle et al., 1998a, b,
157 2003). In the present work, twenty-one samples were selected to represent the various mafic
158 lithologies and alteration types (Table 1): 3 samples are from the UPAZ, 5 from the LPAZ, 6
159 from the MZ, 4 from the UD, and 3 from the LD. All of them are background alteration
160 samples, while veins and alteration halos were avoided.
161
162 **3. Analytical techniques**
163
164 For N analyses, between 40 to 70 mg of fine, homogeneous sample powder was embedded in
165 platinum foil and loaded in quartz tubes prepared with pre-purified reactants (Cu, CuO and
166 CaO). The samples were pre-heated at 300°C under vacuum during one night and then
167 saturated with O_2 pressure generated with CuO heated to 900°C. These steps allow removing
168 any organic contamination and/or atmospheric N_2 adsorbed on the powder surface. The tubes
169 were then sealed under vacuum and N was extracted by a combustion step at temperature of
170 950 or 1050°C during 6 h (Busigny et al., 2005b). A comparison of the combustion at 950 and
171 1050°C for 6 samples shows identical N concentration and isotope composition, suggesting
172 that N was fully extracted at temperature > 950°C (see also results part, below). Nitrogen was
173 purified and separated from other volatiles (mainly H_2O and CO_2) using Cu, CuO and CaO
174 (Kendall and Grim, 1990). It was then quantified as dinitrogen N_2 by capacitance manometry

in ultra-high vacuum line and its isotope analysis was performed on a triple-collector static vacuum mass spectrometer, allowing the measurement of nanomole quantities of N_2. Nitrogen isotopic composition was expressed in the usual δ notation as, $\delta^{15}N_{sample}$ (‰) = $[(^{15}N/^{14}N)_{sample}/(^{15}N/^{14}N)_{standard} -1]\times1000$, where the standard is atmospheric N_2. The quantity of N in the analytical blank was low (0.65 ± 0.30 nmol) relative to samples (> 7 nmol), and its isotopic composition averaged -3.7 ± 2.7 ‰ (2σ). The N concentrations and $\delta^{15}N$ values reported here were corrected from the blank contribution. The precisions determined from external reproducibility on internal and international standards were better than ±8 % and ±0.5 ‰ for nitrogen content and isotopic composition respectively.

For oxygen isotope analyses, 4 to 10 mg of bulk rock powders were loaded in Ni tubes under vacuum and reacted overnight with bromine pentafluoride (BrF_5) at 550°C (Clayton and Mayeda, 1963). The dioxygen produced from the reaction was separated and analyzed on a Thermo-Finnigan™ Delta+XP mass spectrometer. During the course of the study, replicate analyses of NBS-28 quartz standard gave a mean value of 9.45 ± 0.1‰ (1SD, n=17), in good agreement with recommended value (9.58 ± 0.09‰; Gonfiantini et al., 1995), thus providing an estimation of the external precision and accuracy of the measurements.

Major element concentration of the 21 samples were measured in bulk rock using ICP-AES at the Service d'Analyses des Roches et des Minéraux (SARM) of the Centre de Recherches Pétrographiques et Géochimiques (CRPG) of Vandoeuvre, France. Analytical precision for all elements can be found at http://www.crpg.cnrs-nancy.fr/SARM.

Whole rock K, Rb, Cs concentrations were analyzed in the Isotope Geochemistry Laboratories of the National Oceanography Centre Southampton. Analyses were performed on a VG Elemental Plasmaquad PQ2+ ICP-MS calibrated against international rock standard reference materials and corrected for isobaric interferences and blanks. In run errors are typically better than 3% RSD except for Cs where very low concentration samples may show ~10% RSD. Samples with Rb concentrations < 0.05 ppm and Cs concentrations <10 ppb are approaching the detection limits of the techniques used with concentrations less than five times blank levels.

4. Results

4.1. Major and trace element concentrations

Major and trace element concentrations of the samples from Hole 504B are given in Table 1. They are similar to values reported by previous studies (*e.g.* Alt et al., 1996a; Bach et al., 2003). SiO_2 and Al_2O_3 contents are very homogeneous within the section, with mean values of 49.1±0.7 and 15.1±0.8 wt% (1σ; n=21), respectively. Bulk Fe_2O_3 and MgO contents also show a limited range, with values averaging 9.7±0.8 and 8.5±0.5 wt% (1σ; n=21), respectively. The concentrations of CaO and Na_2O average 12.6±0.9 and 2.0±0.4 wt% respectively. Loss on ignition (LOI) is more variable (0.6 to 3.2 wt%; avg. 1.5±0.7 wt%) and is not related to depth in the crust. In contrast, the concentrations of K, Rb and Cs show a systematic decrease with increasing depth in the crust (Table 1; Fig. 2).

4.2. Nitrogen concentration and isotope composition

Nitrogen content and isotope composition of the samples from Hole 504B are reported in Table 2. Six of the 21 samples were duplicated by combustion at temperatures of 950 and 1050°C. The good reproducibility between duplicates confirms that N was completely extracted by heating at temperature ≥ 950°C. Nitrogen content and $\delta^{15}N$ value vary from 1.4 to 14.1 ppm and -0.9 to +7.3 ‰, respectively, a range similar to other altered oceanic basalts (Busigny et al., 2005a; Li et al., 2007) and Mesozoic ophiolites (Bebout et al., 2018). Figure 2 illustrates downhole variations of bulk rock N contents and $\delta^{15}N$ values in Hole 504B. Nitrogen contents show a global decrease with increasing depth (Fig. 2d). The two deepest samples have the lowest N-contents (~ 1.5 ppm) and are only slightly enriched compared to the average of fresh degassed MORB (~1.1 ppm; Sakai et al., 1984; Exley et al., 1987; Marty et al., 1995). Our N concentrations are higher than those obtained by Erzinger and Bach

(1996) on Hole 504B basalts (gray squares in Fig. 2d). The N concentrations of Hole 504B basalts do not correlate with K_2O, Na_2O or $CaO+Na_2O$ concentrations, although N-rich samples also have high K contents (Fig. 3). In contrast to N concentrations, the N isotopic composition does not show a global trend with depth but some oscillation around a mean value (Fig. 2e). The average N isotope composition calculated for the complete section is 3.0 ± 2.2 ‰ (1 SD), and overlaps modern oceanic sediments (most values from 4 to 6 ‰, but total range from 2.5 to 16.6 ‰; *e.g.* Tesdal et al., 2013). The N isotope composition does not correlate with N concentration (Fig. 4a).

4.3. Oxygen isotope composition

The oxygen isotope composition of altered basalts from Hole 504B varies over a large range, with $\delta^{18}O$ values between 3.57 and 7.79‰ (average of 5.7±1.1‰, 1σ; n=16). The depth profile displays a global decrease of $\delta^{18}O$ values with increasing depth, as already observed in previous works (Barrett and Friedrichsen, 1982; Alt et al., 1986a, 1989, 1996; Kawahata et al., 1987; Kusakabe et al., 1989; Mengel and Hoefs, 1990; Agrinier et al., 1995). A comparison of previous and present data shows a good match of the $\delta^{18}O$-depth trends (Fig. 2f). The upper volcanic zone is enriched in ^{18}O compared with typical mantle values and fresh basaltic crust ($\delta^{18}O$ ~ 5.5‰; *e.g.* Eiler et al., 2000) whereas the lower sheeted dike complex exhibits low $\delta^{18}O$ values (Fig. 2f). We emphasize that there is a good positive correlation between $\delta^{18}O$ values and N concentrations (Fig. 4b).

5. Discussion

5.1. Ubiquitous N enrichment during alteration of oceanic basalts

The present data can be used to re-assess the N geochemical behavior in altered basalts from Hole 504B, and provide evidence for ubiquitous N enrichment during alteration of oceanic

crust. All N concentrations measured here are higher than those previously determined by Erzinger and Bach (1996). Although analyses were not performed exactly on the same samples, the trend of N content with depth allows a comparison between samples collected at similar depths and indicates that N contents measured by Erzinger and Bach are lower by more than one order of magnitude (Fig. 2d). This difference likely originates from an artifact related to their analytical technique. Since the original publication of Erzinger and Bach (1996), it has been demonstrated that the use of molybdenum crucible for heating the samples leads to incomplete recovery of N. Indeed, laboratory experiments have shown that high amounts of gaseous nitrogen (> 80%) are soluble in hot molybdenum (Yokochi and Marty, 2006) and molybdenum crucibles or wrapping foil should be avoided during the extraction and quantification of N from rock samples. Instead the use of platinum is recommended for N thermal extraction (Boyd and Pillinger, 1990; Yokochi and Marty, 2006). Moreover, the incomplete recovery of N is associated with modification of the N isotope composition and previous studies using molybdenum must be considered with caution. Numerous N data on terrestrial and extraterrestrial samples should probably be re-evaluated, particularly for those with N content at the ppm-level such as terrestrial basalts and peridotites (*e.g.* Mohapatra and Murty, 2000; 2002) or meteorites (*e.g.* Murty and Marti, 1993; Mathew et al., 2000, 2005).

Nitrogen contents in altered basalts from Hole 504B vary from 1.4 to 14.1 ppm, and decrease with increasing depth. The two deepest samples have N content (~1.4 ppm) similar to fresh degassed MORB from other sites in the oceanic crust (~1.1 ppm; Sakai et al., 1984; Exley et al., 1987; Marty et al., 1995). All other samples from Hole 504B have N content significantly higher than fresh MORB, indicating that N was added to the ocean crust during hydrothermal alteration. If the deepest samples are used as a reference of the background level of unaltered N to evaluate the degree of enrichment during alteration, then N is enriched by at least one order of magnitude. Therefore, the present data reconcile the apparent discrepancy among former studies, with all data now indicating that N is incorporated into the rock, rather than being leached, during interaction with external fluids (Hall, 1989; Busigny et al., 2005a; Li et al., 2007; Bebout et al., 2018; this study; cf. Erzinger and Bach, 1996). All analyses of

oceanic basalts altered by seawater have concentrations in a limited range from 1.3 to 18.2 ppm (Busigny et al., 2005; Li et al., 2007; this study). These samples, including those from the present study, represent typical background alteration but to date only two veins have been analyzed (Busigny et al., 2005a). The two veins showed N content of several hundreds of ppm (354 and 491 ppm), suggesting that a large portion of the N present in the altered upper crust may be carried in secondary minerals (*e.g.* K-rich celadonite and Na-rich pyroxene; Busigny et al., 2003) contained in veins. Further studies should therefore evaluate the vein contribution to the total N amount of the crust.

5.2. Factors controlling the N enrichment in altered oceanic basalts

On the basis of N concentration and isotope composition, the sources of secondary N enrichment can be attributed to deep seawater (*e.g.* NO_3^- or N_2 dissolved in seawater with $\delta^{15}N$ of +5‰ and 0‰ respectively), sediments intercalated in basalt layers ($\delta^{15}N$~4 to 8‰), and/or mantle degassed N ($\delta^{15}N$~-5‰), reduced abiotically during hydrothermal alteration (Busigny et al., 2005a; Li et al., 2007). The positive $\delta^{15}N$ values observed in Hole 504B samples (except one sample at -0.9‰) supports that secondary N was derived from deep seawater or from NH_4^+ released by organic matter diagenesis in the overlying sediments.

To our knowledge, no N isotope data are available for the sediments cored in Hole 504B but a previous study of ODP Legs 170 and 205 on the Costa Rica convergent margin reported $\delta^{15}N$ values between 2.4 to 8.5‰ (Li and Bebout, 2005), within the present range of variation. Although the N speciation in altered basalts from Hole 504B is speculative, N is likely in the form of NH_4^+, which according to similarities in charge and ionic radius, substitutes for K^+, Na^+ and/or Ca^{2+} (Honma and Itihara, 1981). Figure 3 shows that none of these element correlates strictly with N in Hole 504B. However, the samples with high N concentrations also display high K concentration (Figs. 2 and 3). Potassium is enriched in rocks from the uppermost 300 m of basement where the K-bearing mica celadonite and Mg-saponite are common alteration phases (Alt et al., 1996a, 1996b; Bach et al., 2003). The concentrations of K are well

316 correlated with those of Rb and Cs (Fig. 2 a,b,c; Fig. 3b), reflecting as for NH_4^+ their
317 substitution with K in celadonite. The high N concentrations in K-rich samples are thus
318 compatible with N occurring as NH_4^+ in altered basalts. Although both K and N concentrations
319 decrease with depth in Hole 504B, the N content decrease is more continuous than for K, Rb
320 and Cs (Fig. 2). The same kinds of decoupled trends were observed for K and N along a depth
321 profile at Site 801 (Li et al., 2007). The decoupling between K and N concentrations indicates
322 that N enrichment in altered basalts is not only controlled by K concentration of the rocks but
323 requires one or several other parameters. For instance, N concentrations of altered basalts may
324 be influenced by local temperature and/or redox conditions, as suggested from highly
325 heterogeneous N contents and $\delta^{15}N$ values in several DSDP/ODP sites (Li et al., 2007). In the
326 upper part of the oceanic crust, the rocks are altered by interaction with seawater, and in some
327 cases chemically evolved, over a wide temperature range as the crust moves away from the
328 ridge. Thus the alteration process represents an aggregate record of fluid-rock interactions
329 over a temperature range (*e.g.* Alt et al., 1986a, 1996a). The correlation observed in Hole
330 504B basalts between $\delta^{18}O$ and N content (r^2=0.73; Fig. 4) suggests that N could be controlled
331 by local physico-chemical conditions. We explore below two possible scenarios for
332 explaining the depth-trend observed in N concentration (Fig. 2d). The first one is related to a
333 progressive evolution of the fluid composition with depth and the second is a temperature
334 control of the N speciation in the fluid.
335
336 *5.2.1. Evolution of the fluid composition with depth*
337
338 The decrease of N concentration with depth in samples from Hole 504B could reflect the
339 chemical evolution of the fluid due to fluid-rock exchanges that leads to the progressive
340 depletion of N. This could have resulted for instance from successive incorporation of N in
341 the rock, leaving the residual fluid depleted in nitrogen. In this case, one would also expect a
342 continuous evolution of the fluid $\delta^{15}N$, as observed in altered basalts from Leg 206 (Busigny et
343 al., 2005a). In contrast, the $\delta^{15}N$ values of altered basalts from Hole 504B do not display any

344 global trend with depth but instead oscillate around a mean value of 3.0 ± 2.0‰ (1SD; Fig.
345 2e). Moreover, a progressive evolution of a unique fluid with depth is not supported by
346 petrological observations documenting a complex multi-stage alteration history (*e.g.* Laverne
347 et al., 1995; Alt et al., 1986b, 1996a). Detailed petrographic description indicated that
348 alteration of the section penetrated by Hole 504B involves multiple phases of fluid-rock
349 reaction from the bare mid-ocean ridge crest to the thick sediment covered site today. At least
350 four stages of alteration occurred in the mineralized zone and the dike section, two stages in
351 the LPAZ, and three stages in the UPAZ. Therefore several fluids with different N isotope
352 compositions possibly interacted with the rocks, implying that N isotope signature recorded in
353 altered basalts integrated these various alteration stages. We conclude that a scenario
354 involving a chemical evolution of a single fluid with depth seems incompatible with
355 petrological and isotopic data on Hole 504B basalts, as well as with the knowledge on the
356 hydrology of the oceanic crust.
357
358 *5.2.2. A temperature control of the N speciation in the fluid*
359
360 The second scenario that we consider is a temperature control of the N speciation in
361 hydrothermal fluids. The evolution of oxygen isotope composition of oceanic basalts altered
362 by seawater has been studied for a long time and is well understood (*e.g.* Taylor, 1977;
363 Gregory and Taylor, 1981; Friedrichsen et al., 1985; Alt et al., 1986a; Kawahata et al., 1987;
364 Kusakabe et al., 1989; Agrinier et al., 1995; Gao et al., 2012). The $\delta^{18}O$ values of altered rocks
365 depend on a number of parameters such as (1) the temperature of alteration, (2) the isotopic
366 composition of the fluid interacting with the rock, (3) the water/rock ratio, (4) whether the
367 fluid-rock interaction happens in closed or open system and (5) the degree of isotopic
368 exchange between fluid and rock. In the case of Hole 504B, the water/rock (W/R) ratio of
369 altered basalts and dolerites (274 to 1350 mbsf) derived from O and Sr isotopes varies
370 between 1 and 5 (Friedrichsen et al., 1985; Kawahata et al., 1987). In contrast, dolerites from
371 the lower section of the sheeted dike complex, 1350 to 1991 mbsf, are characterized by lower
372 W/R ratios, mostly between 0.2 and 0.5 (Kusakabe et al., 1989; Agrinier et al., 1995). These

low W/R ratios are related to the lower permeability of the deeper rocks in the Sheeted Dike Complex (Alt et al., 1996a). Using the method developed by Taylor (1977), we have modeled the $\delta^{18}O$ of altered basalts for various W/R ratios and alteration temperatures (Fig. 5). We assumed that the initial isotopic compositions of the basalts and seawater were 5.5 and 0‰ respectively, and that the water-rock interaction happened in a closed system. Overall, the strong decrease in O isotope composition with depth, from ^{18}O-enriched (~7.9‰) to ^{18}O-depleted values (~3.5‰), mainly reflects a temperature increase (Fig. 5). Together with the correlation between $\delta^{18}O$ value and N content, this suggests that the N geochemical behavior during alteration of basalts is controlled primarily by temperature variation. One possibility is that N speciation in the fluid, and thus availability for incorporation in secondary minerals, is controlled by temperature. It was shown that NH_4^+ can be stable in hydrothermal fluid at low temperature (<200°C) (Olofsson, 1975; Butterfield et al., 1997; Busigny et al., 2005a; Bourbonnais et al., 2012), thus suggesting that it represents a possible candidate explaining N enrichment in altered basalts. However, NH_4^+ in the fluid is in equilibrium with NH_3 and at high temperature (>200°C), NH_3 is efficiently transformed to N_2 and H_2 (Brown et al., 2018). We can thus hypothesize the following reaction chain, from left to right members, to illustrate the evolution of the hydrothermal fluid for increasing temperature:

$$2NH_4^+ \rightleftarrows 2NH_3 + 2H^+ \rightleftarrows N_2 + 6H_2 + 2H^+ \qquad \text{(Eq. 1)}$$

Figure 6 reports the temperature dependence of the equilibrium constant for the transformation of NH_3 to N_2 and H_2 (Brown et al., 2018). It shows that NH_3 is stable ($K_p > 1$) at relatively low temperatures (< 200°C) but becomes unstable ($K_p < 1$) at temperatures greater than 200°C. It is likely that NH_3 and NH_4^+ were both present in the low-T fluid and were thus partially enriched in the forming alteration phases, but then progressively disappeared with increasing temperature. A similar scenario has also been proposed from the study of hydrothermally altered gabbros from the French-Italian Alps (Busigny et al., 2018).

5.3. Implication for the recycling of N in "warm" subduction zones

401

402 The fate of N in subduction environments can be evaluated from the study of metamorphic
403 rocks in paleo-subduction zones (Bebout and Fogel, 1992; Mingram and Brauer, 2001;
404 Busigny et al., 2003; Halama et al., 2010, 2012; Bebout et al., 1997, 2013) but also from the
405 comparison of N fluxes input by subducting slabs with those output by volcanic arcs (*e.g.*
406 Fischer et al., 2002; Hilton et al., 2002; Zimmer et al., 2004; Mitchell et al., 2010; Li et al.,
407 2005, 2007). These approaches have led in the past to the conclusion that N can either be
408 efficiently lost (Bebout and Fogel, 1992) and quantitatively recycled to the surface *via* arc
409 volcanism (Fischer et al., 2002) or, on the contrary, largely transferred to the deep mantle
410 (Busigny et al., 2003; Li and Bebout, 2005; Li et al., 2007). These opposite conclusions can
411 be reconciled if the geothermal gradient of the subducting slab is taken into consideration
412 (Bebout et al., 1999; Busigny et al., 2003; Mitchel et al., 2010) because N as well as other
413 volatiles can be lost from the slab and migrate into the mantle wedge under high geothermal
414 gradients (> 13°C/km), whereas N can be retained in the subducting slab under lower
415 geothermal gradients (< 10°C/km). Moreover, it can be noted that Fischer et al. (2002) did
416 not consider reasonable estimates of the amount of N entering the subduction zone in
417 sediments but this has been re-estimated in later work (Li and Bebout, 2005). The studies of
418 subduction-zone metamorphic rocks have in general shown that, except in unusually warm
419 margins, the bulk of the initially subducted N bound into silicate minerals such as clays, then
420 micas, can be retained to depths approaching those beneath volcanic fronts (Busigny et al.,
421 2003; Bebout et al., 2013). However, there is no exposed metamorphic record of sediments or
422 altered oceanic crust that was present beneath an active arc. Thermal models indicate
423 significant heating of slabs over the 80-120 km depth range, due to exposure of the slabs and
424 sediments to the convecting part of the mantle wedge (*e.g.* Syracuse et al., 2010). A nitrogen
425 loss could therefore occur during this heating, eventually involving devolatilization and/or
426 partial melting. Mass balance approach based on the fluxes input and ouput in a specific
427 subduction zone can further help to characterize the N behavior in this type of environment.
428 The volcanic arc in Central America is a perfect site to build a global mass balance in a
429 "warm" subduction zone because N fluxes emitted by volcanoes (Fischer et al., 2002; Hilton

et al., 2002; Zimmer et al., 2004) and input by subducting sediments (Li and Bebout, 2005) have already been estimated in previous studies. The Central America margin is regarded as being non-accretionary, thus we do not need to consider accretion as a means of removing some of the sediment from the subducting section (see House et al., 2019, for a different situation in the Sunda margin). Some underplating of sediment could occur at greater depths but this effect cannot be estimated from the present knowledge. The data obtained here on Hole 504B provide the N concentration distribution within the upper crust, thus allowing us to include the upper mafic crust in the mass balance calculation of the Central America margin.

In altered basalts from Hole 504B, N concentration shows an exponential decrease with depth (Fig. 7), which can be described by the following equation:

$$N(z) = A.e^{-Bz} \qquad \text{(Eq. 2)}$$

with N(z) the N concentration, z the depth, and A and B two parameters determined by fitting the data in Figure 7. We can then calculate the flux of N input in Central American subduction zone by upper mafic crust as,

$$\phi_N = \int_0^z N(z).\rho.L.r.dz \qquad \text{(Eq. 3)}$$

where ρ is the density of upper oceanic crust, L is the length of the plate subducting in Central America, and r is the subduction rate. Combining equations 2 and 3 gives,

$$\phi_N = (\rho.L.r)\int_0^z A.e^{-Bz}dz \qquad \text{(Eq. 4)}$$

which can finally be solved and written as,

$$\phi_N = (\rho.L.r).\left[\frac{A}{B}\times(1-e^{-Bz})\right] \qquad \text{(Eq. 5)}$$

In order to compare our results to previous studies (Fischer et al., 2002; Hilton et al., 2002; Zimmer et al., 2004; Li and Bebout, 2005), we adopted the average subducting rate (r) and trench length (L) used by Li and Bebout (2005) of 85 mm/yr and 1100 km, respectively. The density of the upper crust is on average 2900 kg/m^3 (Carlson and Raskin, 1984). Considering a thickness of upper oceanic crust of 2 km, the flux of N transferred to the subduction is ~2.9×10^9 g/yr. It should be noted here that this value represent a lower estimate since breccias, veins and alteration halos have not been included in our mass balance. Comparison of the N

458 input and output fluxes for the Central American subduction zone (Table 3) shows that altered
459 basalts from the upper crust represent more than 35% of the total flux of N released by arc
460 volcanoes in Central America (8.2×10^{9} g/yr; Hilton et al., 2002). However, in comparison
461 with the sedimentary flux (1.3×10^{10} g/yr; Li and Bebout, 2005), the upper basaltic crust is a
462 minor reservoir (~20% of the total N input). Note, however, that there is presently no data for
463 the lower mafic and ultramafic crust subducting in Central America yet. Although mafic and
464 ultramafic rocks from intact crust formed at fast and intermediate spreading rates likely have
465 very low N concentrations (Yokochi et al., 2009; Halama et al., 2010, 2012) comparable to
466 the deeper rocks in Hole 504B, gabbroic rocks make up a significant volume of the ocean
467 crust (*e.g.* 4 km of gabbros in a typical crustal section). The total flux of N input by sediments
468 and upper oceanic crust in Central American trench amounts ~16×10^{9} g/yr although this is
469 likely to be significantly higher if phyllosilicate vein minerals and breccia cements are
470 accounted for. Our estimated flux is at least twice the flux of N degassed by arc volcanoes
471 (Hilton et al., 2002; Table 3). This suggests that in "warm" subduction zone like Central
472 America, up to 50% of the subducted N may be transferred to the deeper mantle. In
473 comparison, in "cold" subduction environments such as the Izu-Bonin-Mariana arc, 80 to
474 95% of the N input is preserved and likely buried in the deep mantle (Mitchell et al., 2010).
475
476 **6. Conclusion**
477
478 In the present contribution, we re-assessed the N concentration, and provide new data of N
479 isotope composition, of altered basaltic rocks from Hole 504B. The N of the upper crust is
480 clearly increased by seawater-rock interactions, a geochemical behavior similar to those
481 observed in other altered oceanic sections (Busigny et al., 2005a; Li et al., 2007). The
482 apparent contradiction with previous analyses by Erzinger and Bach (1996) likely derives
483 from their use of molybdenum crucible for heating the samples in vacuum line.
484 Whole rock basalt N concentrations decrease with depth, from ~15 ppm in the upper basalts
485 down to ~1 ppm in the deepest dolerites, the latter analyses being similar to fresh, unaltered
486 degassed oceanic crust (~1 ppm). In contrast, N isotope composition does not show specific

depth trend and displays a relatively large range around +3.0 ± 2.2‰, similar to sedimentary composition. The N concentration is well correlated with bulk-rock $\delta^{18}O$ values, which likely indicates an evolution of N speciation in hydrothermal fluid with increasing temperature. If the correlation between N content and $\delta^{18}O$ is verified in various DSDP/ODP sites, then $\delta^{18}O$ values could be used as a proxy to estimate the concentration of N content in the oceanic crust in general.

Finally, mass balance calculation on subduction zones supports that the fate of N in subducted slab is dependent on geothermal gradient of the subduction zone, as suggested by earlier studies. In "cold" subduction like most modern environments, N is predominantly preserved in the slab and does not return to the surface *via* arc volcanism. In contrast, in "warm" subduction, N is strongly released but as much as 50% may still be preserved in the slab and be transferred to the deep mantle. Once again, the temperature appears as the essential parameter controlling the N behavior. These findings will need to be taken into consideration in future modeling of the N geodynamic cycles for prediction of the atmosphere evolution and reconstruction of the N distribution among Earth's reservoirs.

Acknowledgements

Colleagues from the Laboratory of Stable Isotope Geochemistry in IPGP are thanked for fruitful discussions. Jean-Jacques Bourrand and Guillaume Landais are acknowledged for their technical assistance with mass spectrometry measurements. VB thanks the SYSTER Program 2014 of the Centre National de la Recherche Scientifique (CNRS) and the Institut Universitaire de France (IUF) for financial support of this project.

References

Agrinier, P., Laverne, C., Tartarotti, P., 1995. Stable isotope ratios (oxygen, hydrogen) and petrology of hydrothermally altered dolerites at the bottom of the sheeted dike complex of Hole 504B. Proc. Ocean Drill Program Sci. Results, 137/140, 99-106.

Alt, J.C., 1995. Subseafloor processes in mid-ocean ridge hydrothermal systems. In: Seafloor Hydrothermal Systems: Physical, Chemical, Biological, and Geological Interactions, Geophys. Monogr. Ser., vol. 91. Edited by S.E. Humphris et al., pp. 85–114, AGU, Washington, D. C., doi:10.1029/ GM091p0085.

Alt, J.C., Teagle, D.A.H., 2000. Hydrothermal alteration and fluid fluxes in ophiolites and oceanic crust. In: Ophiolites and Oceanic Crust: New Insights From Field Studies and the

Ocean Drilling Program, Edited by Y. Dilek et al., Spec. Pap. Geol. Soc. Am., 349, 273–282, doi:10.1130/0-8137- 2349-3.273.

Alt, J.C., Muehlenbachs, K., Honnorez, J. 1986a. An oxygen isotopic profile through the upper kilometer of the oceanic crust DSDP Hole 504B, Earth Planet. Sci. Lett. 80, 217–229.

Alt, J.C., Honnorez, J., Laverne, L., Emmermann, R., 1986b. Hydrothermal alteration of a 1 km section through the upper oceanic crust, DSDP Hole 504B: The mineralogy, chemistry, and evolution of seawater-basalt interactions. J. Geophys. Res. 91, 10,309-10,335.

Alt, J.C., Anderson, T.F., Bonnell, L., Muehlenbachs, K., 1989. Mineralogy, chemistry, and stable isotopic compositions of hydrothermally altered sheeted dikes: ODP Hole 504B, Leg 111. In Becker, K., Sakai, H., et al., Proc. ODP, Sci. Results, 111: College Station, TX (Ocean Drilling Program), 27-40.

Alt, J.C., Laverne, C., Vanko, D., Tartarotti, P., Teagle, D.A.H., Bach, W., Zuleger, E., Erzinger, J., Honnorez, J., 1996a. Hydrothermal alteration of a section of upper oceanic crust in the eastern equatorial Pacific: A synthesis of results from DSDP/ ODP Legs 69, 70, 83, 111, 137, 140, and 148 at Site 504B. Proc. Ocean Drill Program Sci. Results, 148, 417–434.

Alt, J.C., Teagle, D.A.H., Laverne, C., Vanko, D., Bach, W., Honnorez, J., Becker, K., Ayadi, M., Pezard, P.A., 1996b. Ridge flank alteration of upper ocean crust in the eastern Pacific: A synthesis of results for volcanic rocks of Holes 504B and 896A, Proc. Ocean Drill. Program Sci. Results 148, 435–452.

Bach, W., Peucker-Ehrenbrink, B., Hart, S.R., Blusztajn, J.S., 2003. Geochemistry of hydrothermally altered oceanic crust: DSDP/ODP Hole 504B – Implications for seawater-crust exchange budgets and Sr- and Pb-isotopic evolution of the mantle. Geochem. Geophys. Geosyst. 4(3), 8904, doi:10.1029/2002GC000419.

Barrett, T.J., Friedrichsen, H., 1982. Strontium and oxygen isotopic composition of some basalts from Deep Sea Drilling Project Hole 504B, Costa Rica Rift, Legs 69, 70. Earth Planet. Sci. Lett 60, 27-38.

Bebout, G.E., 2013. Chemical and isotopic cycling in subduction zones. In Rudnick R. L. (ed.) The Crust, Treatise on Geochemistry (eds. H. D. Holland and K. K. Turekian, Second Edition), Elsevier-Pergamon, Oxford.

Bebout, G.E., Fogel, M.L., 1992. Nitrogen-isotope compositions of metasedimentary rocks in the Catalina Schist, California: implications for metamorphic devolatilization history. Geochim. Cosmochim. Acta 56, 2839-2849.

Bebout, G.E., Ryan, J.G., Leeman, W.P., Bebout, A.E., 1999. Fractionation of trace elements by subduction-zone metamorphism – effect of convergent-margin thermal evolution. Earth Planet. Sci. Lett. 171, 63-81.

Bebout, G.E., Banerjee, N.R., Izawa, M.R.M., Kobayashi, K., Lazzeri, K., Ranieri, L.A., Nakamura, E., 2018. Nitrogen concentrations and isotopic compositions of seafloor-altered terrestrial basaltic glass: Implications for astrobiology. Astrobiology 18, 330-342.

Bourbonnais, A., Lehmann, M.F., Butterfield, D.A., Juniper, S.K., 2012. Subseafloor nitrogen transformations in diffuse hydrothermal vent fluids of the Juan de Fuca Ridge evidenced by the isotopic composition of nitrate and ammonium. Geochem. Geophys. Geosyst., 13, Q02T01, doi:10.1029/2011GC003863.

564 Boyd, S.R., Pillinger, C.T., 1990. Determination of the abundance and isotope composition of
565 nitrogen within organic compounds: a sealed tube technique for use with static vacuum
566 mass spectrometers. Meas. Sci. Technol. 1, 1176-1183.

567 Brown, T.E.B., LeMay H.E., Bursten, B.E., Murphy, C., Woodward, P., Stoltzfus, M.E.,
568 2018. Chemistry: The Central Science, 14th Edition. Pearson, Boston, USA, pp. 1248.

569 Busigny, V., Cartigny, P., Philippot, P., Ader, M., Javoy, M., 2003. Massive recycling of
570 nitrogen and other fluid-mobile elements (K, Rb, Cs, H) in a cold slab environment:
571 Evidences from HP to UHP oceanic metasediments of the Schistes Lustrés nappe (Western
572 Alps, Europe). Earth Planet. Sci. Lett. 215, 27-42.

573 Busigny, V., Laverne, C., Bonifacie, M. 2005a. Nitrogen content and isotopic composition of
574 oceanic crust at a superfast spreading ridge: A profile in altered basalts from ODP Site
575 1256, Leg 206. Geochem. Geophys. Geosyst. 6, Q12O01, doi:10.1029/2005GC001020.

576 Busigny, V., Ader, M., Cartigny, P., 2005b. Quantification and isotopic analysis of nitrogen
577 in rocks at the ppm level using sealed-tube combustion technique: a prelude to the study of
578 altered oceanic crust. Chem. Geol. 223, 249–258.

579 Busigny V., Chen J.B., Philippot P., Moynier F., 2018. Insight into hydrothermal and
580 subduction processes from copper and nitrogen isotopes in oceanic metagabbros. Earth and
581 Planetary Science Letters 498, 54-64.

582 Butterfield, D.A., Jonasson, I.R., Massoth, G.J., Feely, R.A., Roe, K.K., Embley, R.E.,
583 Holden, J.F., McDuff, R.E., Lilley, M.D., Delaney, J.R., 1997. Seafloor eruptions and
584 evolution of hydrothermal fluid chemistry. Philos. Trans. R. Soc. London A 355, 369–386.

585 Carlson, R.L., Raskin, G.S., 1984. Density of the ocean crust. Nature 311, 555-558.

586 Cartigny, P., Marty, B., 2013. Nitrogen isotopes and mantle geodynamics: The emergence of
587 life and the atmosphere-crust-mantle connection. Elements 9, 356-366.

588 Eiler, J.M., Schiano, P., Kitchen, N., Stolper, E.M., 2000. Oxygen-isotope evidence for
589 recycled crust in the sources of mid-ocean-ridge basalts. Nature 403, 530-534.

590 Erzinger, J., Bach, W., 1996. Downhole variation of nitrogen in hole 504B: preliminary
591 results. In Proceeding of the Ocean Drilling Program, Scientific Results, Vol. 148 (eds. J.
592 C. Alt, H. Kinoshita, L. B. Stokking, and P. J. Michael), pp. 3-7.

593 Exley, R.A., Boyd, S.R., Mattey, D.P., Pillinger C.T., 1987. Nitrogen isotope geochemistry of
594 basaltic glasses: implications for mantle degassing and structure. Earth Planet. Sci. Lett.
595 81, 163-174.

596 Fischer, T.P., Hilton, D.R., Zimmer, M.M., Shaw, A.M., Sharp, Z.D., Walker, J.A., 2002.
597 Subduction and recycling of nitrogen along the Central American margin. Science 297,
598 1154-1157.

599 Gao, Y., Vils, F., Cooper, K.M., Banerjee, N., Harris, M., Hoefs, J., Teagle, D.A.H., Casey,
600 J.F., Elliot, T., Laverne, C., Alst, J.C., Muehlenbachs, K., 2012. Downhole variation of
601 lithium and oxygen isotopic compositions of oceanic crust at East Pacific Rise, ODP Site
602 1256, Geochem. Geophys. Geosyst., 13, Q10001, doi:10.1029/2012GC004207.

603 Gonfiantini, R., Stichler, W., Rozanski, K., 1995. Standards and intercomparison materials
604 distributed by the International Atomic Energy Agency for stable isotope measurements.
605 IAEA-TECDOC-825, 13-30.

606 Gregory, R.T., Taylor, H.P., 1981. An oxygen isotope profile in a section of Cretaceous
607 oceanic crust, Samail Ophiolite, Oman: Evidence for $\delta^{18}O$ buffering of the oceans by deep

(> 5km) seawater-hydrothermal circulation at Mid-Ocean Ridges. Journal of Geophysical Research 86, 2737-2755.

Halama, R., Bebout, G.E., John, T., Schenk, V., 2010. Nitrogen recycling in subducted oceanic lithosphere: the record in high- and ultrahigh-pressure metabasaltic rocks. Geochim. Cosmochim. Acta 74, 1636-1652.

Halama, R., Bebout, G.E., John, T., Scambelluri, M., 2012. Nitrogen recycling in subducted mantle rocks and implications for the global nitrogen cycle. International Journal of Earth Sciences, doi:10.1007/s00531-012-0782-3.

Hall, A., 1989. Ammonium in spilitized basalts of southwest England and its implications for the recycling of nitrogen. Geochem. J. 23, 19-23.

Hilton, D.R., Fischer, T.P., Marty, B., 2002. Noble gases and volatile recycling at subduction zones. In Noble gases in geochemistry and cosmochemistry (Eds. Porcelli, D., Ballentine, C. J., Wieler, R.), Rev. Mineral. Geochem. 47, Washington DC, pp. 319-370.

Honma, H., Itihara, Y., 1981. Distribution of ammonium in minerals of metamorphic and granitic rocks. Geochim. Cosmochim. Acta 45, 983–988.

Honnorez, J., Alt, J.C., Honnorez-Guerstein, B.-M., Laverne, C., Muehlenbachs, K., Ruiz, J., Saltzman, E., 1985. Stockwork-like sulfide mineralization in young oceanic crust: Deep Sea Drilling Project Hole 504B. Initial Rep. Deep Sea Drill. Proj. 83, 263–282.

House, B.M., Bebout, G.E., Hilton, D.R., 2019. Carbon cycling at the Sunda margin, Indonesia: A regional study with global implications. Geology 47, 483-486.

Kawahata, H., Kusakabe, M., Kikuchi, Y., 1987. Strontium, oxygen and hydrogen isotope geochemistry of hydrothermally altered and weathered rocks in DSDP Hole 504B, Costa Rica Rift. Earth Planet. Sci. Lett. 85, 343-355.

Kusakabe, M., Shibata, T., Yamamoto, M., Mayeda, S., Kagami, H., Honma, H., Masuda, H., Sakai, H., 1989. Petrology and isotope characteristics (H, O, S, Sr, and Nd) of basalts from Ocean Drilling Program Hole 504B, Leg 111, Costa Rica Rift. In Becker, K., Sakai, H., et al., Proc. ODP, Sci. Results, 111. College Station, TX (Ocean Drilling Program), 47-60.

Laverne, C., Vanko, D.A., Tartarotti, P., Alt, J.C., 1995. Chemistry and geothermometry of secondary minerals from the deep sheeted dike complex, DSDP/OPD Hole 504B. In: Erzinger, J., Becker, K., Dick, H.J.B., Stocking, L.B. (Eds.), Proc. Ocean Drill. Program: Sci. Results, vol. 137/140. Ocean Drilling Program, College Station, TX, pp. 167–189.

Laverne, C., Agrinier, P., Hermitte, D., Bohn, M., 2001. Chemical fluxes during hydrothermal alteration of a 1200-m long section of dikes in the oceanic crust, DSDP/ODP Hole 504B. Chemical Geology 181, 73-98.

Li, L., Bebout, G.E., Idleman, B.D., 2007. Nitrogen concentration and $\delta^{15}N$ of altered oceanic crust obtained on ODP Legs 129 and 185: Insights into alteration-related nitrogen enrichment and the nitrogen subduction budget. Geochim. Cosmochim. Acta 71, 2344-2360.

Li, L., Bebout, G.E., 2005. Carbon and nitrogen geochemistry of sediments in the Central American convergent margin: Insights regarding subduction input fluxes, diagenesis, and paleoproductivity. J. Geophys. Res. 110, B11202, doi:10.1029/2004JB003276.

Marty, B., 1995. Nitrogen content of the mantle inferred from N_2-Ar correlation in oceanic basalts. Nature 377, 326-329.

651 Mathew, K.J., Palma R.L., Marti, K., Lavielle B., 2000. Isotopic signatures and origin of
652 nitrogen in IIE and IVA iron meteorites. Geochim. Cosmochim. Acta 64, 545-557.

653 Mathew, K.J., Mart, K., Kim, Y., 2005. Nitrogen in chondrite metal. Geochim. Cosmochim.
654 Acta 69, 753-762.

655 Mengel, K., Hoefs, J., 1990. Li-δ^{18}O-SiO_2 systematics in volcanic rocks and mafic lower
656 crustal granulite xenoliths. Earth and Planetary Science Letters 101, 42-53.

657 Mingram, B., Bräuer, K., 2001. Ammonium concentration and nitrogen isotope composition
658 in metasedimentary rocks from different tectonometamorphic units of the European
659 Variscan Belt. Geochim. Cosmochim. Acta 65, 273-287.

660 Mitchell, E.C., Fischer, T.P., Hilton, D.R., Hauri, E.H., Shaw, A.M. et al., 2010. Nitrogen
661 sources and recyling at subduction zones: Insights from the Izu-Bonin-Mariana arc.
662 Geochem. Geophys. Geosys. 11, Q02X11, doi:10.1029/2009GC002783.

663 Mohapatra, R.K., Murty, S.V.S., 2000. Search for the mantle nitrogen in the ultramafic
664 xenoliths from San Carlos, Arizona. Chem. Geol. 164, 305-320.

665 Mohapatra, R.K., Murty, S.V.S., 2002. Nitrogen and noble gas isotopes in mafic and
666 ultramafic inclusions in the alkali basalts from Kutch and Reunion - implications for their
667 mantle sources. J. Asian Earth Sci. 20, 867-877.

668 Murty, S.V.S., Marti, K., 1993. Nitrogen isotopic signatures in Cape York: Implications for
669 formation of Group IIIA irons. Geochim. Cosmochim. Acta 58, 1841–1848.

670 Olofsson, G., 1975. Thermodynamic quantities for the dissociation of the ammonium ion and
671 for the ionization of aqueous ammonia over a wide temperature range, J. Chem.
672 Thermodyn., 7, 507–514.

673 Sakai, H., Des Marais, D.J., Ueda, A., Moore, J.G., 1984. Concentrations and isotope ratios of
674 carbon, nitrogen and sulfur in ocean-floor basalts. Geochim. Cosmochim. Acta 48, 2433-
675 2441.

676 Staudigel, H., 2003. Hydrothermal Alteration Processes. In: The Crust (Eds Holland H,
677 Turekian K.), Treatise on geochemistry vol. 3, Elsevier, New York, pp 511–535.

678 Syracuse, E.M., van Keken, P.E., Abers, G.A., 2010. The global range of subduction zone
679 thermal models. Physics of the Earth and Planetary Interiors 183, 73-90.

680 Taylor, H.P., 1977. Water/rock interactions and the origin of H_2O in granitic batholiths. J.
681 Geol. Soc. London 133, 509–558, doi:10.1144/gsjgs.133.6.0509.

682 Teagle, D.A.H., Alt, J.C., Halliday, A.N., 1998a. Tracing the chemical evolution of fluids
683 during hydrothermal recharge: Constraints from anhydrite recovered in ODP Hole 504B,
684 Earth Planet. Sci. Lett., 155, 167-182.

685 Teagle, D.A.H., Alt, J.C., Halliday, A.N., 1998b. Tracing the evolution of hydrothermal fluids
686 in the upper oceanic crust: Sr isotopic constraints from DSDP/ODP Holes 504B and 896A.
687 In: Modern Ocean-Floor Processes and the Geological Record, R.A. Mills and K. Harrison,
688 eds, Geol. Soc. Lond. Spec. Pub. 148, pp. 81-97.

689 Tesdal, J.E., Galbraith, E.D., Kienast, M., 2013. Nitrogen isotopes in bulk marine sediment:
690 linking seafloor observations with subseafloor records. Biogeosciences 10, 101–118.

691 Vanko, D.A., Laverne, C, 1998. Hydrothermal anorthitization of plagioclase within the
692 magmatic/hydrothermal transition at mid-oceanic ridges: examples from deep sheeted

693 dikes (Hole 504B, Costa Rica Rift) and a sheeted dike root zone (Oman ophiolite). Earth
694 Planet. Sci. Lett. 162, 27-43.

695 Yokochi, R., Marty, B., 2006. Fast chemical and isotopic exchange of nitrogen during
696 reaction with hot molybdenum. Geochem. Geophys. Geosyst. 7, Q07004,
697 doi:10.1029/2006GC001253.

698 Yokochi, R., Marty, B., Chazot, G., Burnard, P., 2009. Nitrogen in peridotite xenoliths:
699 lithophile behavior and magmatic isotope fractionation. Cosmochim. Acta 73, 4843–4861.

700 Zimmer, M.M., Fischer, T.P., Hilton, D.R., Alvarado, G.E., Sharp, Z.D., Walker J.A., 2004.
701 Nitrogen systematics and gas fluxes of subduction zones: Insights from Costa Rica arc
702 volatiles, Geochem. Geophys. Geosyst., 5, Q05J11, doi:10.1029/2003GC000651.
703
704

Figure caption

Figure 1. Map illustrating the location of DSDP/ODP Hole 504B, as well as other drill sites, referred in the main text, near Central American convergent margin (modified from Busigny et al., 2005).

Figure 2. Depth profiles of (A) potassium, (B) rubidium, (C) cesium and (D) nitrogen concentrations (ppm), as well as (E) nitrogen (‰ vs Air) and (F) oxygen (‰ vs SMOW) isotope compositions in altered basalts from Hole 504B (black circles). The main lithological variations are reported on the left of the figure: volcanic zone (VZ), transition zone (TZ) and sheeted Dike Complex (SDC). The main alteration zones are also reported on the left of the figure: low-temperature oxidizing (LTO), low-temperature reducing (LTR), mineralized (M), upper dikes (UD), lower dikes (LD). Horizontal dashed lines represent the depth range of the five alteration zones as indicated on the right end side of the figure: Upper Pillow Alteration Zone (UPAZ), Lower Pillow Alteration Zone (LPAZ), Mineralized Zone (MZ), Upper Dikes (UD), Lower Dikes (LD). D: the gray squares represent the data reported by Erzinger and Bach (1996) using Mo crucible for N extraction. The black vertical line represents N concentration of the fresh (non-altered) mid ocean ridge basalts (MORB). E: the gray bar represents the average $\delta^{15}N$ value of mantle nitrogen (-5‰; Cartigny and Marty, 2013). F: the gray diamonds correspond to a compilation of data from the literature (Barrett and Friedrichsen, 1982; Alt et al., 1986a, 1989, 1996; Kawahata et al., 1987; Kusakabe et al., 1989; Mengel and Hoefs, 1990; Agrinier et al., 1995), and illustrates similar trend to the one measured in our study (black circles). The gray bar represents the average $\delta^{18}O$ value of the mantle (+5.5 ‰; Eiler et al., 2000).

Figure 3. Relationships between N, K, Rb, Na_2O and $CaO+Na_2O$ concentrations in altered basalts from Hole 504B.

Figure 4. Relations between N concentrations (ppm) and N (‰ vs Air) and O (‰ vs SMOW) isotope compositions in altered basalts from Hole 504B.

Figure 5. Calculated $\delta^{18}O$ values of altered basalts equilibrated with seawater at different temperature (50 to 500°C) and water/rock ratios (W/R). The calculation assumes constant $\delta^{18}O$ value of seawater at ~0‰ and O isotope fractionation between water and rock defined as $\Delta_{water\text{-}rock} = 2.5(10^6)/T^2 - 3.70$ (*e.g.* Gregory and Taylor, 1981). The range of water/rock ratio reported for Hole 504B in the literature is indicated by the light gray band (Friedrichsen et al., 1985; Kawahata et al., 1987; Kusakabe et al., 1989; Agrinier et al., 1995).

Figure 6. Equilibrium constant (K_P, expressed from gas pressure) as a function of temperature for the reaction of ammonia formation from N_2 and H_2 (Brown et al., 2018). Ammonia is favored at low temperature (<200°C) whereas N_2 is more stable at temperatures >200°C.

Figure 7. Relation between N concentration (ppm) and depth in the oceanic crust (mbb: meter below basement) for altered basalts from Hole 504B. The data are better fitted by an exponential law (R^2=0.82) than a linear regression (R^2=0.74, not shown).

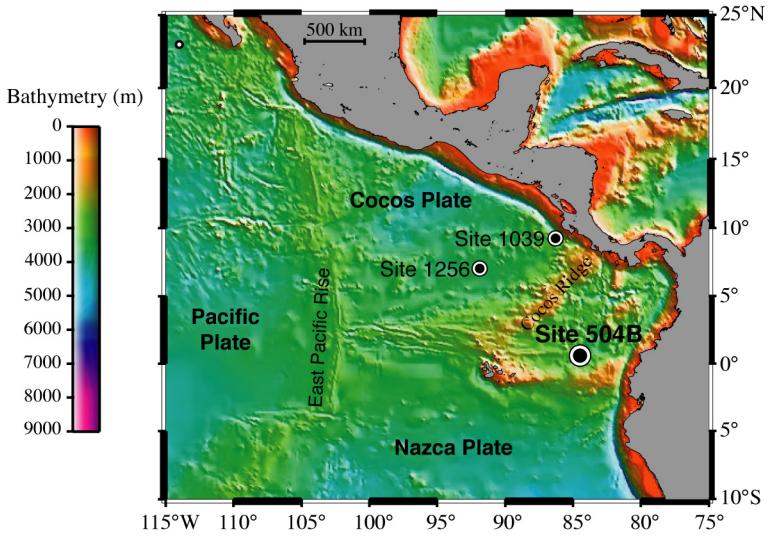


Figure 1

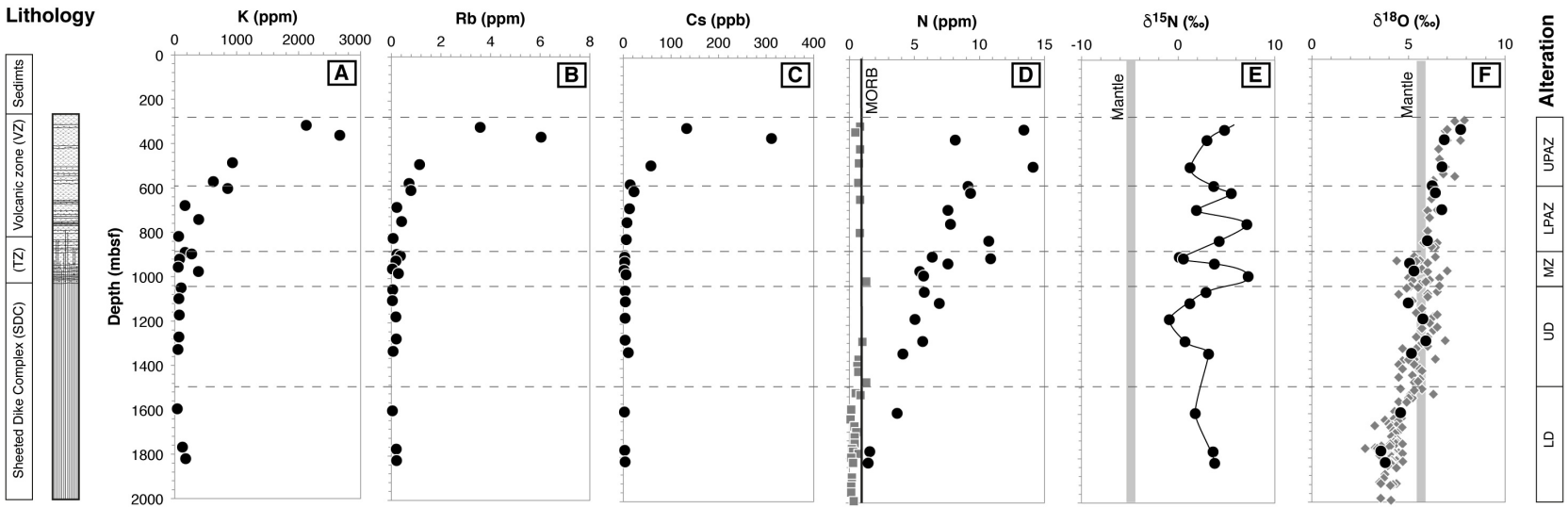

Lithology
Sediments
Volcanic zone (VZ)
(TZ)
Sheeted Dike Complex (SDC)
Depth (mbsf)
K (ppm)
Rb (ppm)
Cs (ppb)
N (ppm)
δ15N (‰)
δ18O (‰)
MORB
Mantle
Mantle
A
B
C
D
E
F
Alteration
UPAZ
LPAZ
MZ
UD
LD

FIGURE 2

762

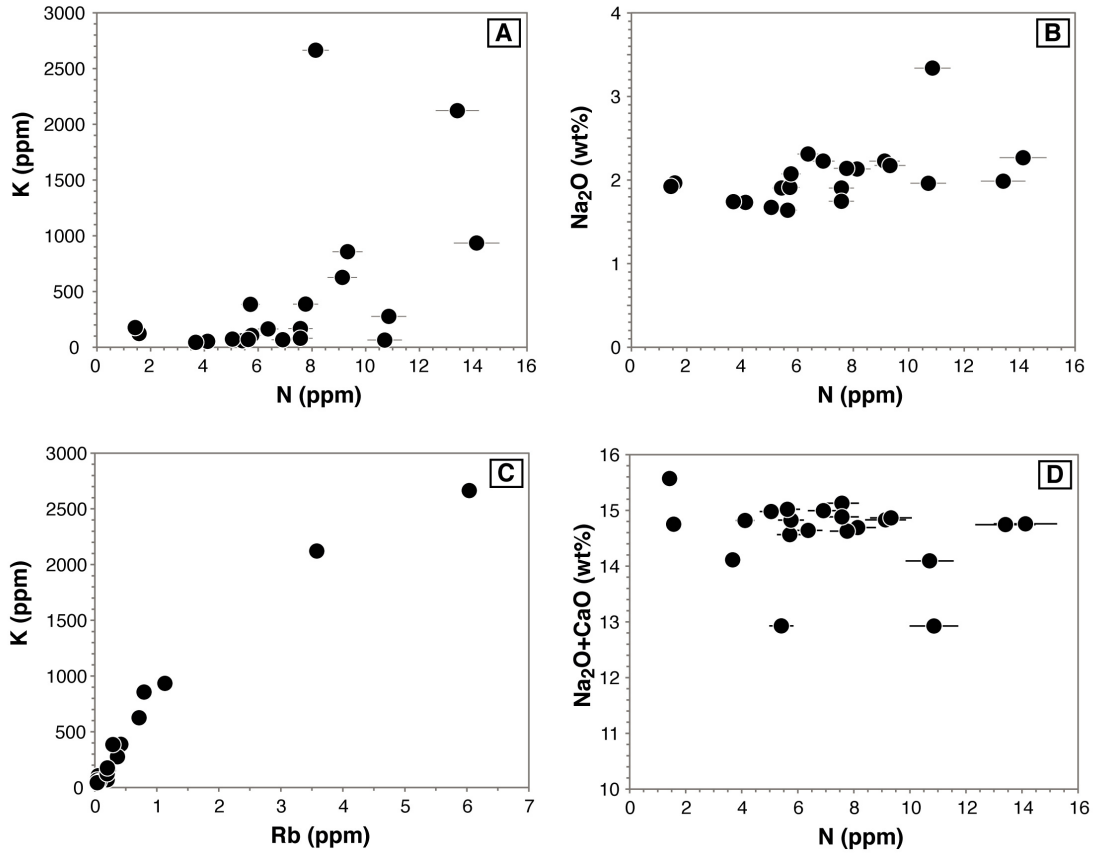


Figure 3

763
764
765
766

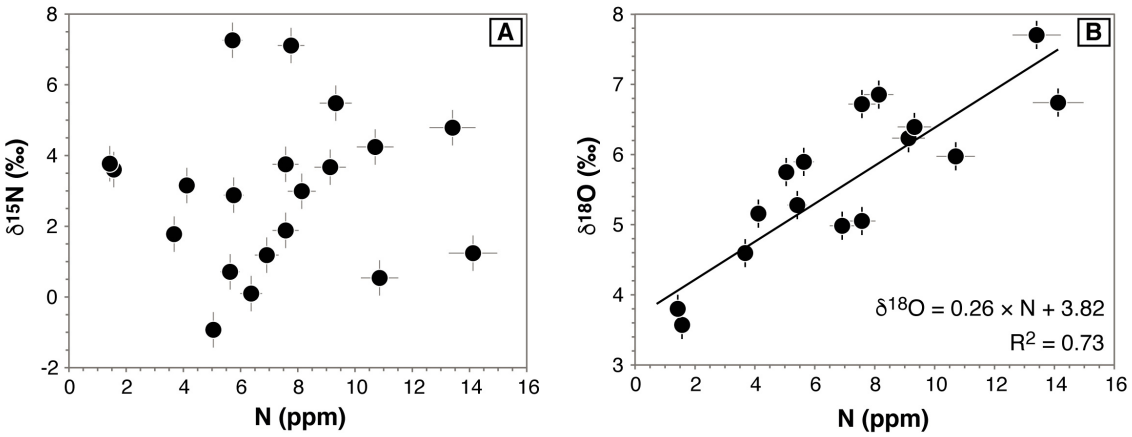


Figure 4

767
768

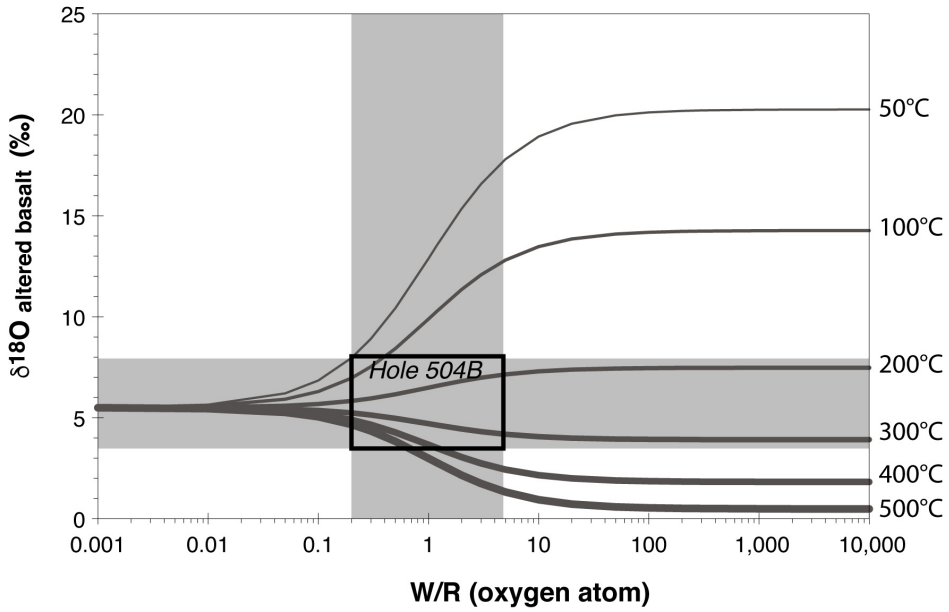


Figure 5

769
770
771

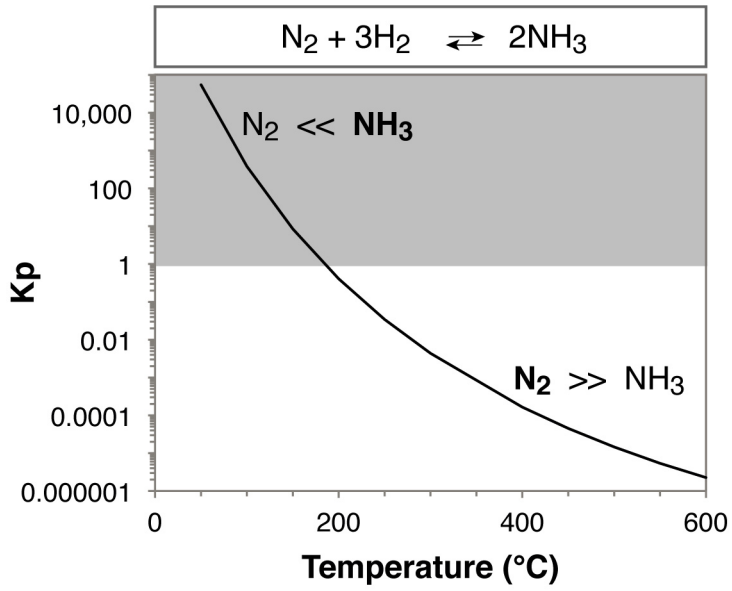


Figure 6

772
773
774
775

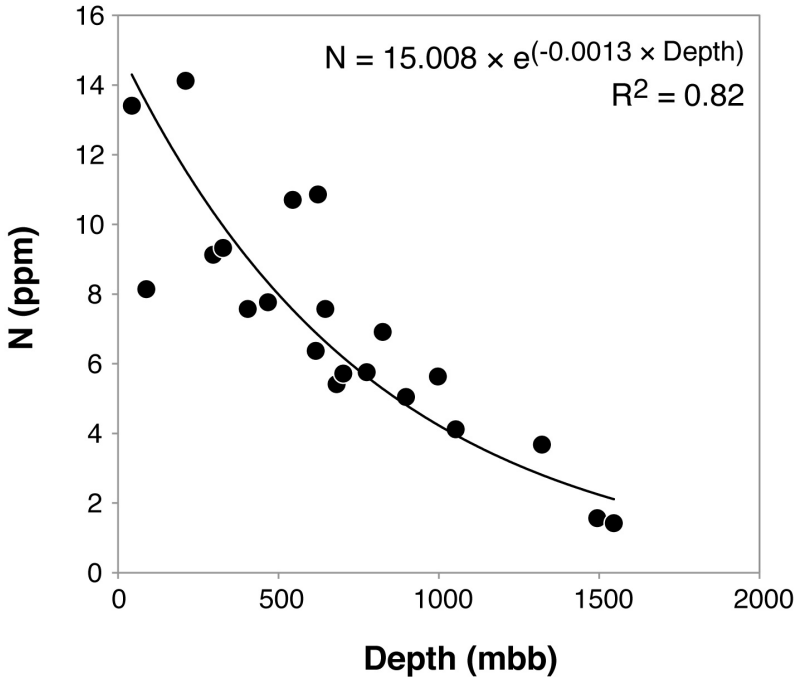


Figure 7

776
777
778

Table 1
Depth, alteration zone, major and trace element concentrations and oxygen isotope composition (‰ vs SMOW) of altered basalts from Hole 504B.

Core-section, Interval (cm)	Depth* (mbsf)	Alteration zone	SiO_2 (wt%)	Al_2O_3 (wt%)	Fe_2O_3 (wt%)	MnO (wt%)	MgO (wt%)	CaO (wt%)	Na_2O (wt%)	TiO_2 (wt%)	P_2O_5 (wt%)	LOI (wt%)	Total (wt%)	K (ppm)	Rb (ppb)	Cs (ppb)	$\delta^{18}O$ (‰)
8-1, 69-72	317.2	UPAZ	48.50	15.71	10.03	0.16	7.72	12.76	1.99	0.86	0.09	0.65	98.63	2122.3	3578.3	132.7	7.70
13-1, 81-84	362.4	UPAZ	48.91	15.01	10.00	0.18	7.94	12.56	2.13	0.96	0.08	1.43	99.51	2664.2	6038.5	311.1	6.85
29-2, 16-19	485.2	UPAZ	49.03	14.71	9.51	0.17	8.41	12.49	2.27	1.00	0.08	1.57	99.32	934.5	1130.7	57.8	6.74
39-1, 62-66	571.2	UPAZ	49.64	15.91	9.25	0.18	7.98	12.60	2.23	0.93	0.09	1.41	100.21	626.1	713.3	14.1	6.23
43-1, 17-19	602.2	LPAZ	50.14	15.14	9.80	0.17	8.50	12.69	2.17	0.90	0.08	1.07	100.67	856.8	794.8	22.6	6.39
52-1, 38-40	678.9	LPAZ	48.79	16.51	8.77	0.15	7.92	13.22	1.91	0.82	0.07	1.36	99.51	167.7	223.8	13.2	6.72
60-1, 46-49	742	LPAZ	49.94	14.69	10.47	0.17	8.57	12.49	2.14	1.05	0.11	0.65	100.27	387.3	419.7	7.8	n.a.
69-1, 95-99	819	LPAZ	48.39	14.14	10.77	0.23	8.36	12.13	1.96	1.08	0.10	1.84	98.98	64.8	65.8	6.5	5.98
77-2, 71-73	890.8	MZ	49.40	14.45	10.85	0.20	8.38	12.33	2.31	1.04	0.10	1.17	100.22	164.1	218.5	3.1	n.a.
78-1, 6-11	897.6	MZ	49.59	14.88	10.25	0.17	8.19	9.59	3.34	0.95	0.09	3.22	100.27	276.7	365.5	2.9	n.a.
81-1, 128-132	920.8	MZ	48.88	14.98	9.73	0.23	8.53	13.14	1.75	0.88	0.09	1.42	99.62	80.6	183.4	3.1	5.05
85-1, 47-49	956	MZ	49.45	14.02	9.89	0.38	8.71	11.02	1.91	0.96	0.08	2.80	99.21	59.1	48.6	1.8	5.28
88-1, 12-16	976.7	MZ	47.48	15.20	9.48	0.23	8.72	12.65	1.91	0.99	0.12	3.03	99.82	384.8	291.3	5.4	n.a.
96-1, 125-127	1049.7	MZ	49.85	14.44	8.83	0.21	8.55	12.75	2.07	0.91	0.08	1.16	98.85	106.6	56.1	3.8	n.a.
101-1, 98-102	1099.5	UD	48.85	14.55	9.56	0.19	8.38	12.77	2.23	0.90	0.07	1.58	99.07	67.2	39.3	4.1	4.99
113-1, 122-126	1172.3	UD	49.80	15.15	10.09	0.17	8.96	13.31	1.67	0.84	0.08	0.70	100.76	72.6	184.3	3.4	5.75
129-2, 23-27	1271.8	UD	48.91	15.97	8.74	0.15	9.93	13.38	1.64	0.69	0.07	1.39	100.87	70.6	199.2	3.5	5.90
137-1, 31-34	1327.4	UD	48.44	15.87	8.96	0.15	8.98	13.09	1.73	0.79	0.07	1.16	99.23	53.5	69.7	10.3	5.16
176R-1, 85-89	1596.1	LD	49.42	14.30	10.82	0.17	7.95	12.37	1.74	0.97	0.08	0.86	98.69	44.1	37.7	2.2	4.60
207R-1, 0-4	1768.4	LD	49.79	14.28	10.71	0.19	8.32	12.79	1.97	1.00	0.09	0.58	99.70	122.9	200.3	3.2	3.57
214R-2, 29-32	1820.4	LD	48.55	16.97	7.88	0.12	9.07	13.65	1.92	0.69	0.06	1.53	100.42	176.6	204.1	3.6	3.80

* mbsf: meters below seafloor; n.a.: not analyzed.
Alteration zones: Upper Pillow Alteration Zone (UPAZ), Lower Pillow Alteration Zone (LPAZ), Mineralized Zone (MZ), Upper Dikes (UD), Lower Dikes (LD).

789

790 Table 2
791 Nitrogen concentration and isotope composition of altered basalts from Hole 504B.

Core-section, Interval (cm)	Piece #	Temp (°C)	N (ppm)	$\delta^{15}N$ (‰)
8-1, 69-72	524	950	13.7	5.1
8-1, 69-72	524	1050	13.2	4.4
			13.4	*4.8*
13-1, 81-84	759	1050	8.1	3.0
29-2, 16-19	1581	1050	14.1	1.2
39-1, 62-66	463	950	9.1	3.7
43-1, 17-19		950	9.2	5.1
43-1, 17-19		1050	9.5	5.8
			9.3	*5.5*
60-1, 46-49	1260	950	7.8	7.1
69-1, 95-99	1547	1050	10.7	4.2
77-2, 71-73	6	950	6.2	-0.1
77-2, 71-73	6	1050	6.5	0.3
			6.4	*0.1*
78-1, 6-11	2	950	10.9	0.5
81-1, 128-132	15	950	7.6	3.8
85-1, 47-49	6b	1050	5.4	n.a.
88-1, 12-16	2A	950	5.9	7.5
88-1, 12-16	2A	1050	5.6	7.0
			5.7	*7.3*
96-1, 125-127	6b	1050	5.8	2.9
101-1, 98-102	10a	1050	6.9	1.2
113-1, 122-126	13	950	5.0	-0.9
129-2, 23-27	1C	950	5.6	0.7
137-1, 31-34	4	1050	4.1	3.2
176R-1, 85-89	16	1050	3.7	1.8
207R-1, 0-4		950	1.5	3.8
207R-1, 0-4		1050	1.6	3.4
			1.6	*3.6*
214R-2, 29-32	7	950	1.4	3.1
214R-2, 29-32	7	1050	1.4	4.5
			1.4	*3.8*

792 Temp: temperature of N extraction from the sample during combustion in quartz sealed-tube.
793 Values in *italic*: mean values of replicate analyses; n.a.: not analyzed.
794 The precision on N content and $\delta^{15}N$ are better than 8% and 0.5‰, respectively.
795
796
797

798

799 Table 3
800 Comparison of the nitrogen fluxes input in and output from Central American subduction zone.

		N flux, g/yr	Method used for estimating N flux	Reference
Output	Volcanic arc	8.2×10^{9}	N_2 degassed in Central American arc	Hilton et al., 2002
	Volcanic arc	3.6×10^{8}	N_2 degassed in Costa Rica only	Zimmer et al., 2004
Input	Sediments	6.4×10^{9}	N concentration assumed for shales (100 ppm) and carbonates (0 ppm)	Fischer et al., 2002
	Sediments	1.3×10^{10}	N concentration measured in sediments from ODP Site 1039	Li and Bebout, 2005
	Upper oceanic crust (2 km)	2.9×10^{9}	N concentration measured in altered basalts from DSDP/ODP Site 504B	This study

801
802